Journal of Biomolecular NMR, **19:** 181–185, 2001.
KLUWER/ESCOM

A graphical method for the analysis of anisotropic rotational diffusion in proteins

Oscar Millet* & Miquel Pons**
Departament de Química Orgànica, Universitat de Barcelona, Martí i Franquès 1-11, E-08028 Barcelona, Spain

Received 7 August 2000; Accepted 12 December 2000

Key words: graphical methods, proteins, relaxation, rotational diffusion tensor anisotropy

Abstract

A graphical method for the analysis of relaxation data is presented. It allows a fast estimation of the range of values of the components of the axially symmetric rotational diffusion tensor that are compatible with the experimental relaxation data. The graphical method clearly shows the contribution of different experimental relaxation parameters to the measured anisotropy. In particular, for proteins with moderate anisotropy, data from at least two N-H bonds forming angles close to 0° and 90° with respect to the principal axis of the rotational diffusional tensor are needed. For very anisotropic systems, combination of different relaxation parameters from a single residue is enough to characterize the local anisotropy.

NMR has become a widely used tool for the study of protein dynamics at different timescales (Palmer et al., 1996). Relaxation data are often analyzed in terms of the model free approach (Lipari and Szabo, 1982a,b), which considers the global and local motions uncorrelated, and leads to a bi-exponential correlation function. For isotropically rotating proteins, the output of the analysis consists in an overall correlation time that describes the rotation of the molecule, a generalized order parameter (S^2) and an internal correlation time (τ_e) for every residue, denoting its degree of independent motion and the spatial restriction for these fluctuations.

Most proteins are better described by an axially symmetric model rather than an isotropic one. Their motion is then described by the two different components of the rotational diffusion tensor ($D_\perp$ and $D_\parallel$), rather than by a single correlation time. The spectral density function for anisotropic overall reorientation of an N-H bond is given by the equation (Woessner, 1962):

$$J(\omega)=S^2\left[\frac{1}{4}\frac{(3\cos^2\theta-1)^2\tau_a}{1+(\omega\tau_a)^2}+\frac{(3\sin^2\theta\cos^2\theta)\tau_b}{1+(\omega\tau_b)^2}+\frac{3}{4}\frac{\sin^4\theta\tau_c}{1+(\omega\tau_c)^2}\right] \quad (1)$$

where $\tau_a^{-1}=D_\perp$, $\tau_b^{-1}=5/6D_\perp+1/6D_\parallel$, $\tau_c^{-1}=1/3D_\perp+2/3D_\parallel$, and θ is the angle between the N-H vector and the main axis of the rotational diffusion tensor. The complete asymmetrical model involves a larger number of parameters in the fitting and for most proteins does not lead to a significant improvement of the model. It will not be considered in the present work.

Different methods can be used for the determination of the anisotropic diffusional tensor in proteins. The R_2/R_1 ratio for a set of nuclear spins can be directly fit to obtain $D_\parallel$ and $D_\perp$ (Tjandra et al., 1995, 1997; Zheng et al., 1995), provided that the 3D structure is known. Residues with larger-than-average values for R_2/R_1 are excluded from the calculation. In a different approach, local diffusion coefficients are derived from relaxation rate constants (Brüschweiler et al., 1995). Relaxation data are fit locally to an isotropic model, obtaining an effective correlation time. These correlation times are then fit to

*Present address: Department of Medical Genetics, Biochemistry, and Chemistry, University of Toronto, Toronto, ON, Canada. E-mail: oscar@pound.med.utoronto.ca
**Correspondence can be addressed to either author. E-mail: mpons@qo.ub.es

an anisotropic model to obtain the components of the diffusion tensor.

In the present communication we present a graphical method for the determination of the rotational diffusion tensor in anisotropic peptides and proteins. A graphical method has been described for the determination of the order parameter and the internal correlation time (Henry et al., 1986; Weaver et al., 1988; Jin et al., 1997, 1998). All the ^{15}N experimental relaxation rates R_i can be expressed as a sum of $J(\omega)$ at characteristic frequencies or, through Equation 1, as a function of $D_\perp$ and $D_\parallel$ and S^2 (Abragam, 1961). For residues with large order parameters, the S^2 dependency can be removed by taking the ratio between two rates measured at the same magnetic field. In all cases, residues belonging to secondary structural elements have been chosen. The ratios of transversal and longitudinal relaxation rates (R_2/R_1) and of transversal and longitudinal cross-correlation rates (η_{xy}/η_z) are both sensitive measures of anisotropy. The latter has the advantage that it is not sensitive to chemical exchange.

In order to graphically characterize the rotational diffusion tensor, the values of $D_\perp$ and $D_\perp/D_\parallel$ that yield a given ratio R_2/R_1or η_{xy}/η_z are represented as contour plots. Contours for $R_i/R_j \pm \Delta$, where R_i/R_j is the observed ratio and Δ represents the experimental uncertainty of R_i/R_j derived from the individual uncertainties of R_i and R_j, define an open area that includes all values of $D_\perp$ and $D_\perp/D_\parallel$ compatible with the experimental data. The solution area becomes well defined when the contour plots of two independent ratios cross each other. Contour plots of different ratios of relaxation rates measured for a single residue cross each other only for very large values of the anisotropy. On the other hand, when contour plots for two N-H groups oriented with different angles θ are represented simultaneously, well-defined sets of solutions are found. The relaxation of an N-H group forming an angle of $\theta = 0°$ will only be affected by rotations perpendicular to the principal axis, but not by rotations around this axis. Thus, the comparison of data from two residues oriented at 0° and 90° from the principal axis of the rotational diffusion tensor should provide the minimum solution area.

As the rotational diffusion tensor is not known a priori, we define the angle θ' with respect to the main axis of the inertia tensor. The ratios R_2/R_1 or η_{xy}/η_z, and the corresponding uncertainties, of two N-H groups with θ' close to 0° and 90° are represented. Statistically it is more probable to find a residue forming an angle of 90° than an angle of 0°.

The method has been tested with proteins having different degrees of anisotropy that had been previously analyzed with different numerical methods. Table 1 compares the range of values of $D_\perp/D_\parallel$ and $D_\perp$ obtained from the graphical analysis with those obtained by numerical minimization. In general there is a good agreement between the graphical and numerical analyses. Some of the graphical analyses are also presented in Figure 1. Contour plots of R_2/R_1 at 9.40 T and 17.62 T for two residues of the N-terminal DNA-binding domain of the 434 repressor (Luginbühl et al., 1997) are shown in Figure 1A. The intersection area, denoting the values of the diffusion tensor compatible with the experimental data, is shaded. Thick lines that show the coordinates of the numerical solution cross well within the allowed area defined graphically. The area of the possible solutions, and therefore the accuracy of the parameters, depends on the experimental uncertainty of the different measurements. In Figure 1B, contours of R_2/R_1 at 18.79 T and R_2/R_1 and η_{xy}/η_z at 11.74 T are plotted for W120 and L111 of *Escherichia coli* ribonuclease H (Kroenke et al., 1998,1999). In this example, the range of allowed values of $D_\perp/D_\parallel$ is determined mainly by R_2/R_1 at 11.74 T. In contrast, η_{xy}/η_z determines the possible values of $D_\perp$. The values of $D_\perp$ and $D_\perp/D_\parallel$ estimated numerically fall, within the limits of their own error bars, in the graphically determined solution space. The graphical analysis for ribonuclease H has been repeated, using different residues that have an angle θ' $\approx 90°$. Residues spread in the plane XY (relative angles $\psi_{(W120/Q72)} = 139°$, $\psi_{(W120/Y39)} = 31°$) define nearly identical regions of the $D_\perp$–$D_\perp/D_\parallel$ space (see Supplementary material, available from the authors on request), indicating that this protein is well described by an axially symmetric model. While it is usually possible to find several NH groups with θ' close to 90°, NH bonds with θ' close to 0° are less abundant. The effect of using data from NH groups with θ' angles different from zero is to increase the area of the allowed region, and therefore to decrease the accuracy of the graphical method. This effect is illustrated using data from ribonuclease H in the Supplementary material (Figure S2).

For the N-terminal domain of enzyme I (Tjandra et al., 1997; Figure 1C), the contours of the ratios R_2/R_1 at 14.09 T alone provide an accurate graphical estimation of the anisotropic diffusion tensor, indicating that one set of data is enough to define the rotational diffusion tensor, provided that the experimental uncertainties are small.

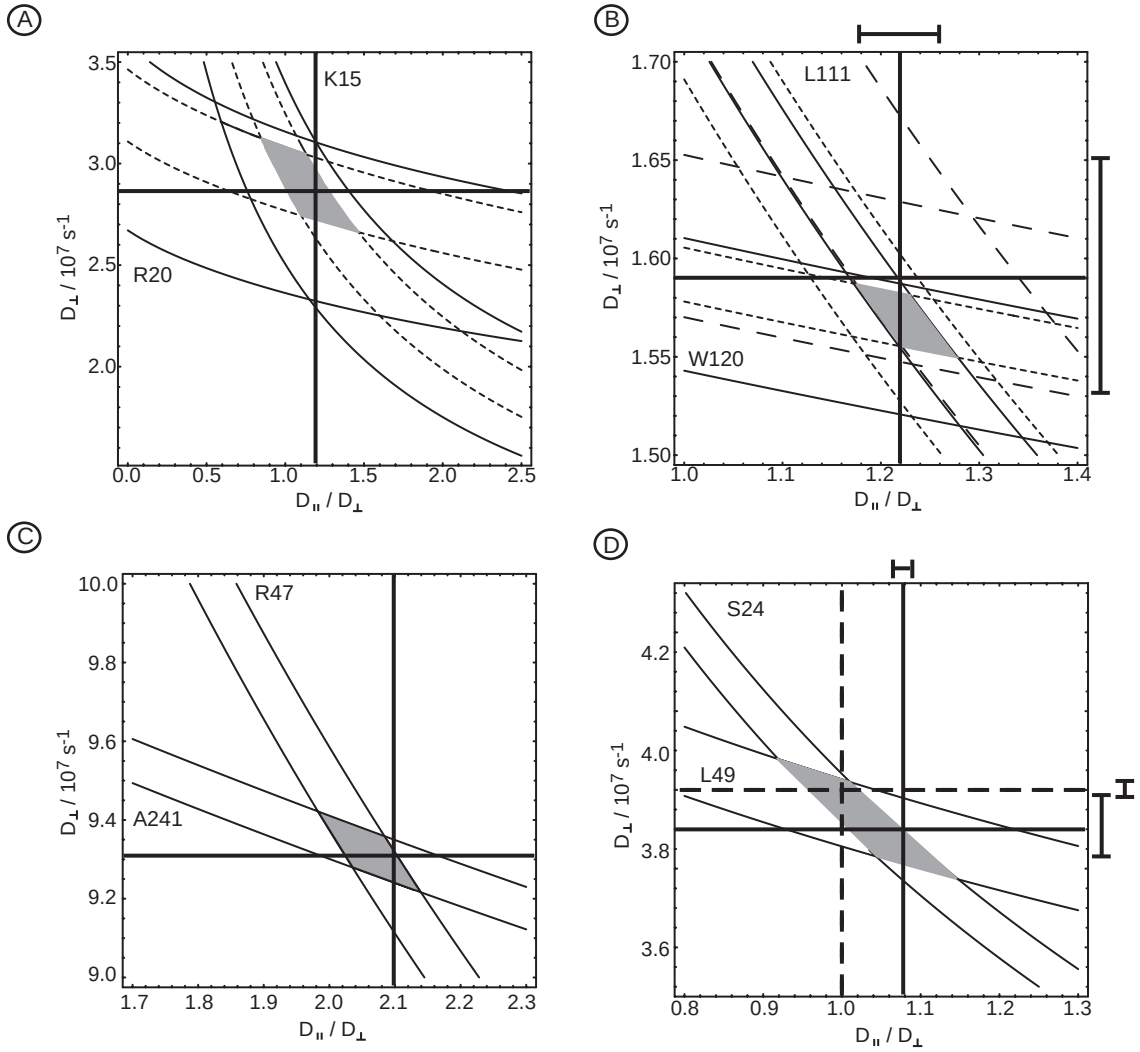

Figure 1. Contour plots of R_2/R_1 or η_{xy}/η_z as a function of the principal values of the rotational diffusion tensor for different proteins. (A) R_2/R_1 at 9.40 T (solid line) and 17.62 T (dashed line) for K15 ($\theta' = 25°$) and R20 ($\theta' = 83°$) of the N-terminal DNA-binding domain of the 434 repressor. (B) R_2/R_1 at 11.74 T (solid line), R_2/R_1 at 18.79 T (dashed line (long dash)) and η_{xy}/η_z at 11.74 T (dashed line (short dash)) for W120 ($\theta' = 89°$) and L111 ($\theta' = 158°$) for *Escherichia coli* ribonuclease H. (C) R_2/R_1 at 14.09 T for R47 ($\theta' = 159°$) and A241 ($\theta' = 86°$) for the N-terminal domain of enzyme I. (D) R_2/R_1 at 11.74 T for L49 ($\theta = 92°$) and S24 ($\theta = 144°$) for calbindin D_{9k}. In all cases perpendicular solid lines correspond to the coordinates of the solution obtained by minimization of a complete relaxation data set. Error bars for these values are shown in the margins of the plot when available. In (D) the dashed coordinates show the numerical solution considering an isotropic model while the solid coordinates correspond to the axially symmetric tensor.

To test the method in the case of low anisotropy, a graphical analysis of the calbindin D_{9k} relaxation data has been performed. These data had been previously analyzed using an isotropic model (Kördel et al., 1992) or an axially symmetrical model (Lee et al., 1997). The results are represented by the dotted and solid coordinates in Figure 1D along with the solution space determined graphically from contour plots of R_2/R_1 at 11.74 T. For this plot, the true rotational tensor previously determined (Lee et al., 1997) was used to calculate the angles θ and to choose the pair of residues to be represented. The graphical analysis using the inertia tensor can be obtained as Supplementary material. The allowed area encloses both the isotropic and the anisotropic solutions. Therefore, for very low anisotropies, restriction of the analysis to pairs of residues does not provide enough resolution to differentiate isotropic from anisotropic diffusion.

Table 1 also shows results for the regulatory domain of troponin C (Gagné et al., 1998) and ubiquitin

Table 1. Comparison of rotational diffusion anisotropy values obtained by graphical and numerical methods

Protein	$D_\perp/D_\parallel$		$D_\perp/10^7$		Residue 1	Residue 2
	(min-max)	(num. anal.)	(min-max)	(num. anal.)	(res/θ')	(res/θ')
DNA-binding domain[a,d]	0.85–1.5	1.20	2.65–3.1	2.87	K20/83°	R15/25°
Ribonuclease H[b,d]	1.18–1.28	1.22	1.55–1.59	1.59	W120/89°	L111/158°
Enzyme I[b,e]	1.98–2.15	2.10	0.92–0.94	0.931	A241/86°	R47/156°
Calbindin D_{9k}[a,e]	0.92–1.15	1.08(1)[c]	3.74–3.97	3.84(3.92)[c]	(L49/92°)[f]	(S24/144°)[f]
Calbindin D_{9k}[a,e]	0.88–1.07	1.08(1)[c]	3.80–4.15	3.84(3.92)[c]	F10/89°	S24/144°
Ubiquitin[a,e]	1.11–1.28	1.17	3.75–3.88	3.83	L69/91°	G35/26°
Troponin C[a,e]	1.00–1.12	1.10	3.21–3.33	3.34	G77/93°	F26/24°
γ-zein	5.00–19.00	12.5	2.0–3.5	2.28	L15/90°	–

[a]Residues chosen correspond to the closest angle to 90° and 0° or 180°, respectively.
[b]NH groups with θ' angles closest to 0° and/or 90° do not belong to a secondary structural element or not all of the experimental data are available. Another residue that fulfills the requirements has been chosen instead.
[c]Value in parentheses corresponds to the isotropic fitting.
[d]PDB file: X-ray crystallographic data.
[e]PDB file: NMR solution structure data.
[f]The value of θ instead of θ' is given for these residues.

(Tjandra et al., 1995). Contour plots for these proteins are similar to those shown in Figure 1 and are included in the Supplementary material.

When the degree of anisotropy is large enough, contour lines for different combination of relaxation parameters from a single residue can cross, giving an independent solution for every residue in the protein. In Figure 2 this is shown for L15 of the N-terminal domain of the γ-zein (Geli et al., 1994), a 48-residue peptide with the repetitive sequence $(VHLPPP)_8$. Previous studies indicated that this domain adopts a polyproline II helical conformation in aqueous solution (Dalcol, 1997). A model free analysis for this protein reflects that the molecule has an axially symmetrical anisotropic motion with a ratio $D_\perp/D_\parallel$ of 12.5 (unpublished results), constituting an excellent candidate for the present graphical approach. The astonishingly large degree of anisotropy obtained for this molecule can be due in part to aggregation effects. Previous studies demonstrate the existence of aggregation at lower concentrations (Dalcol, 1997). Figure 2 shows the contour lines corresponding to R_2/R_1 at 7.04 T and 11.74 T and the ratio NOE(7.04 T)/NOE(11.74 T). The limits of the solution area are determined from the three different combinations used, indicating that all data are relevant in the determination of the coefficients of the rotational diffusional tensor. A comparison between the numerical and graphical values is presented in Table 1.

In conclusion, we have presented a new graphical approach for the determination of the rotational diffusion tensor. It provides a fast estimation of the degree of anisotropy reflected by the relaxation data. These values can be used to obtain a starting point for further numerical minimization protocols or to

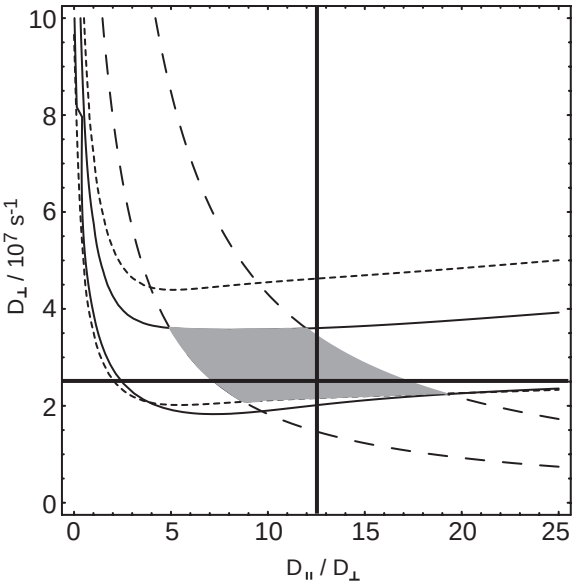

Figure 2. Graphical analysis of the local anisotropy of L15 in the N-terminal domain of γ-zein. Contour plots of R_2/R_1 at 7.04 T (solid line), 11.74 T (dashed line (short dash)) as well as NOE(7.04)/NOE(11.74) (dashed line (long dash)) have been used. The shaded area defines all the values of the rotational diffusion tensor compatible with the experimental data. Due to the large degree of anisotropy, the allowed values of $D_\perp$ and $D_\perp/D_\parallel$ can be defined by contour plots of different pairs of experimental relaxation parameters from a single residue.

determine if an anisotropic model is required to fit the relaxation data. The graphical method presented also provides a visual estimation of the contribution of different experimental data sets to the measured anisotropy and of the uncertainty in the parameters derived from experimental errors.

Acknowledgements

We are indebted to Pau Bernadó for his assistance in the calculation of the inertia tensor from the pdb files. This work has been supported by funds from the Spanish Ministerio de Educación y Cultura (PB97-0933) and the Generalitat de Catalunya (Centre de Referència de Biotecnologia and Grup de Recerca Consolidat). We acknowledge the use of the NMR facilities of the Serveis Científico-tecnics of the University of Barcelona.

Supplementary material

Three contour plots for ribonuclease H using NH groups with different values of θ' (θ' close to 90°), four contour plots for ribonuclease H with NH groups with different values of θ' (θ' close to 0°), and three contour plots for calbindin D_{9k}, ubiquitin and troponin C can be obtained from the authors on request.

References

Abragam, A. (1961) *Principles of Nuclear Magnetism*, Clarendon Press, Oxford, U.K.

Brüschweiler, R., Liao, X. and Wright, P.E. (1995) *Science*, **268**, 886–889.

Dalcol, I. (1997) *Synthesis and structural studies of proline-rich peptides with helical structure*, Ph.D. Thesis, Universitat de Barcelona, Barcelona, Spain.

Gagné, S.M., Tsuda, S., Spyracopoulos, L., Kay, L.E. and Sykes, B.D. (1998) *J. Mol. Biol.*, **278**, 667–686.

Geli, M.I., Torrent, M. and Ludevid, M.D. (1994) *Plant Cell*, **6**, 1911–1922.

Henry, G.D., Weiner, J.H. and Sykes, B.D. (1996) *Biochemistry*, **25**, 590–598.

Jin, D., Andrec, M., Montelione, G. and Levy, R.M. (1998) *J. Biomol. NMR*, **12**, 471–492.

Jin, D., Figueirido, F., Montelione, G. and Levy, R.M. (1997) *J. Am. Chem. Soc.*, **119**, 6923–6924.

Kördel, J., Skelton, N.J., Akke, M., Palmer, A.G. and Chazin, W.J. (1992) *Biochemistry*, **31**, 4856–4866.

Kroenke, C.D., Loria, J.P., Lee, L.K., Rance, M. and Palmer III, A.G. (1998) *J. Am. Chem. Soc.*, **120**, 7905–7915.

Kroenke, C.D., Rance, M. and Palmer, A.G. (1999) *J. Am. Chem. Soc.*, **121**, 10119–10125.

Lee, L.K., Rance, M., Chazin, W.J. and Palmer, A.G. (1997) *J. Biomol. NMR*, **9**, 287–298.

Lipari, G. and Szabo, A. (1982a) *J. Am. Chem. Soc.*, **104**, 4546–4559.

Lipari, G. and Szabo, A. (1982b) *J. Am. Chem. Soc.*, **104**, 4559–4570.

Luginbühl, P., Pervushin, K.V., Iwai, H. and Wüthrich, K. (1997) *Biochemistry*, **36**, 7305–7312.

Palmer, A.G., Williams, J. and McDermott, A. (1996) *J. Chem. Phys.*, **100**, 13293–13310.

Tjandra, N., Feller, S.E., Pastor, R.W. and Bax, A. (1995) *J. Am. Chem. Soc.*, **117**, 12562–12566.

Tjandra, N., Garrett, D.S., Gronenborn, A.G., Bax, A. and Clore, G.M. (1997) *Nat. Struct. Biol.*, **4**, 443–449.

Weaver, A.J., Kemple, M.D. and Prendergast, F.G. (1988) *Biophys. J.*, **54**, 1–15.

Woessner, D.E. (1962) *J. Chem. Phys.*, **37**, 647–654.

Zheng, Z., Czaplicki, J. and Jardetzky, O. (1995) *Biochemistry*, **34**, 5212–5223.